Hindawi Publishing Corporation
Journal of Nanomaterials
Volume 2012, Article ID 767128, 7 pages
doi:10.1155/2012/767128

Research Article

Electronic Structure of the $CuCl_2(100)$ Surface: A DFT First-Principle Study

Sherin A. Saraireh[1] and Mohammednoor Altarawneh[2,3]

[1] *Physics Department, Faculty of Sciences, Al-Hussein bin Talal University, P.O. Box 20, Ma'an, Jordan*
[2] *Chemical Engineering Department, Faculty of Engineering, Al-Hussein bin Talal University, P.O. Box 20, Ma'an, Jordan*
[3] *Priority Research Centre for Energy, Faculty of Engineering and Built Environment, The University of Newcastle, Callaghan, NSW 2308, Australia*

Correspondence should be addressed to Sherin A. Saraireh, sh2002jo@yahoo.com

Received 13 March 2012; Accepted 11 June 2012

Academic Editor: Shafiul Chowdhury

First-principle density functional theory (DFT) and a periodic-slab model have been utilized to investigate the structure of the $CuCl_2(100)$ surface. Structural parameters of the bulk $CuCl_2$ are reported and compared with the experimental values. The structure of the $CuCl_2(100)$ is calculated using a (2×2) supercell. Structural parameters in terms of bond lengths and bond angle are calculated. Electronic properties of the $CuCl_2(100)$ surface are investigated by calculating the density of state (DOS) and the projected density of state for a slab containing five layers.

1. Introduction

Copper plays a prominent role in many fields. This is primarily due to its unique mechanical properties and excellent electrical and thermal conductivity. Its applications spans heating and cooling piping, heat exchanging, electrical appliances, architecture, and catalysis [1–6].

Adsorption of halides on metallic surfaces is of particular importance due to their relevance for many industrial processes and its role in the formation of notorious environmental pollutants such as dioxins [7]. Central to a comprehensive understanding of various phenomena such as corrosion, electrodeposition, and catalytic cycles is addressing adsorption of chlorine on copper surfaces on a precise atomic-scale.

Motivated by its diverse application, the chlorine-copper interaction has attracted great deal of experimental [8–14] and theoretical [15–18] studies. Mounting experimental evidence shows a strong interaction between Cl and Cu atoms as evident from electron diffraction (LEED) [8], normal-incident X-ray standing wave (NIXSW) [9], surface-extended X-ray adsorption fine structure (SEXAFS) [10, 11], shadow-cone-enhanced secondary-ion mass spectrometry (SIMS) [6, 12], and Scanning Tunnelling microscopy (STM) [13, 14] methods. STM studies found that the chlorine molecules adsorb dissociatively on the Cu(111) surface, leading to formation of various well-ordered phases. It is also found that Cl atoms prefer to adsorbs onto face-centered cubic (fcc) hollow positions over the hexagonal close-pack (hcp) hollow, bridge, and top positions [13, 18].

Computational data for the Cl/Cu(111) system based on cluster [15] or a periodic DFT-based calculation [16, 17, 19] has been presented by different groups Doll and Harrison [16], Migani et al. [17], and Peljhan and Kokalj [19]. It was found that the preferred adsorption of the Cl atoms is the face-centered cubic (fcc) [16]. Peljhan et al. presented an extensive DFT calculation of Cl adsorption on Cu(111), considering a wide range of Cl coverages ranging from 1/16 to 1 ML. The strong interaction between Cl and Cu atoms results in the formation of two distinctive different materials; namely, CuCl and $CuCl_2$. The crystal structure of the $CuCl_2$ follows a base-centered monoclinic space group C2/m [20–22]. As demonstrated by Burns and Hawthrone [23]. Cu atoms are positioned in an axially distorted octahedral

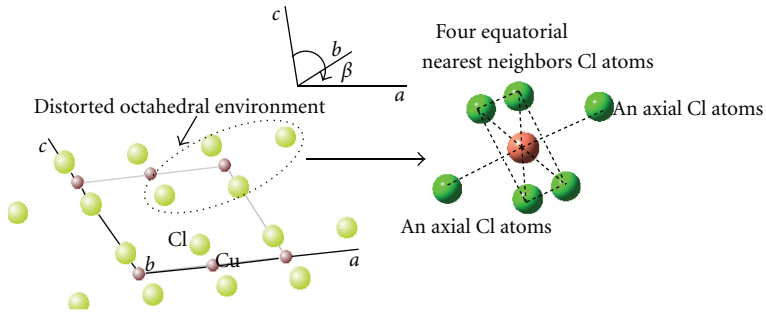

Figure 1: Unit cell of $CuCl_2$. In online version, green circle represent Cl atoms while red and violet circles represent Cu atom.

environment with four equatorial nearest neighbors Cl atoms and two axial Cu atoms.

First-principle simulation, based on density functional theory (DFT), is now one of the key tools for studying and developing a key understanding of solid surfaces. DFT calculations can provide an atomic-based insight into the detailed bonding arrangement of structures, their energetic stability, and charge densities. To this end, this contribution investigates the electronic structure of the Copper (II) chloride, $CuCl_2$, mainly in the (100) surface orientation.

2. Methodology

The calculations reported in this paper have been performed using the plane wave pseudopotential density functional theory (DFT) method as implemented in the VASP program [24–27]. The generalized gradient approximation (GGA) for exchange and correlation as developed by Perdew and Wang (PW91) [28] was used to perform the spin-polarized calculations. Projector augmented wave (PAW) potentials [24, 25, 29] are used to represent the ionic potentials. A unit cell comprising four atomic layers has been employed together with a vacuum thickness of at least 14 Å to separate each slab from its neighboring images along the z-direction (normal to the surface). The three top-most layers of the slab were allowed to fully relax. The Brillouin-Zone (BZ) integrations were performed using automatic generation of $(3 \times 3 \times 1)$ and $(5 \times 5 \times 1)$ k-point set of Monkhorst-Pack random sampling [30]. Total energy was converged to an accuracy of 1×10^{-3} eV. Deployed energy cut-off was set at 300 eV. The choice of this value, stems from the maximum value of the kinetic-energy for the Cl and Cu atoms, that is, 280 and 273 eV, respectively.

3. Results

3.1. Bulk Properties. $CuCl_2$ forms a base-centered Monoclinic Bravies lattice. As shown in Figure 1, each Cu atom is in an axially distorted octahedral environment with four equatorial nearest neighbors Cl atoms and two axial Cl atoms. The lattice constants were determined (as illustrated in Table 1) by plotting the variation in the energy with respect to the volume of the unit cell of bulk $CuCl_2$. The lattice constants of bulk $CuCl_2$ are compared with calculated data in reference [19] and experiment data in references [23, 31] in Table 1. This comparison shows that our results are in a relative good agreement with those of earlier experiment and computational studies.

Table 1: Comparison of our calculated properties of the bulk $CuCl_2$ bulk with previous calculated data [19] and experiment data [23, 31].

Reference	Lattice constant			
	a (Å)	b (Å)	c (Å)	β (deg.)
This work	7.35	3.40	7.20	117
Previous calculation (ref. [19])	7.52	3.35	7.29	119
Experiment (ref. [23, 31])	6.90	3.30	6.82	122

The calculated total density of states (DOS) and atomic-projected DOS (pDOS) for bulk $CuCl_2$ are presented in Figure 2; Figure 2(a) shows the Density of state (DOS) of the $CuCl_2$ bulk, while Figure 2(b) shows the projected density of state for Cu atom and Figure 2(c) shows the projected density of state for Cl atom.

There are two distinct bands in the valence region (Figure 2(a)). The Cu band (predominantly Cu 3d and little contributions of Cu (3p and 4s)) occupies the region (0 to −5) eV, and the Cl band (predominantly Cl (3s and 3p)) occupies that of (−14 to −15) eV. The surface state band resides just above the Fermi level where two regions are highlighted. The first one is in the region from 3.0 to 7.0 eV, while the second one is from 7.5 to 9.0 eV. The first region above the Fermi level is predominantly the empty state Cu 4s and the contribution in this region from Cu 3p and Cl (3s and 3p) is minimal (see Figures 2(b) and 2(c)). The second region above the Fermi level is predominantly the state Cu (3d and 3p) and Cl (3s and 3p).

3.2. $CuCl_2$(100) Surface. A supercell of the $CuCl_2$(100) is constructed from the optimized bulk unitcell and also based on the data in [21, 22, 32]; the unit cell is shown in Figure 3. This unit cell is a base-centered Monoclinic with one Cu atom located in the center of each base and four Cl atoms in the corner of each base. The Cu atom has four nearest neighbors Cl atoms in the same plane (plane of a and b) and two Cl atoms in c direction.

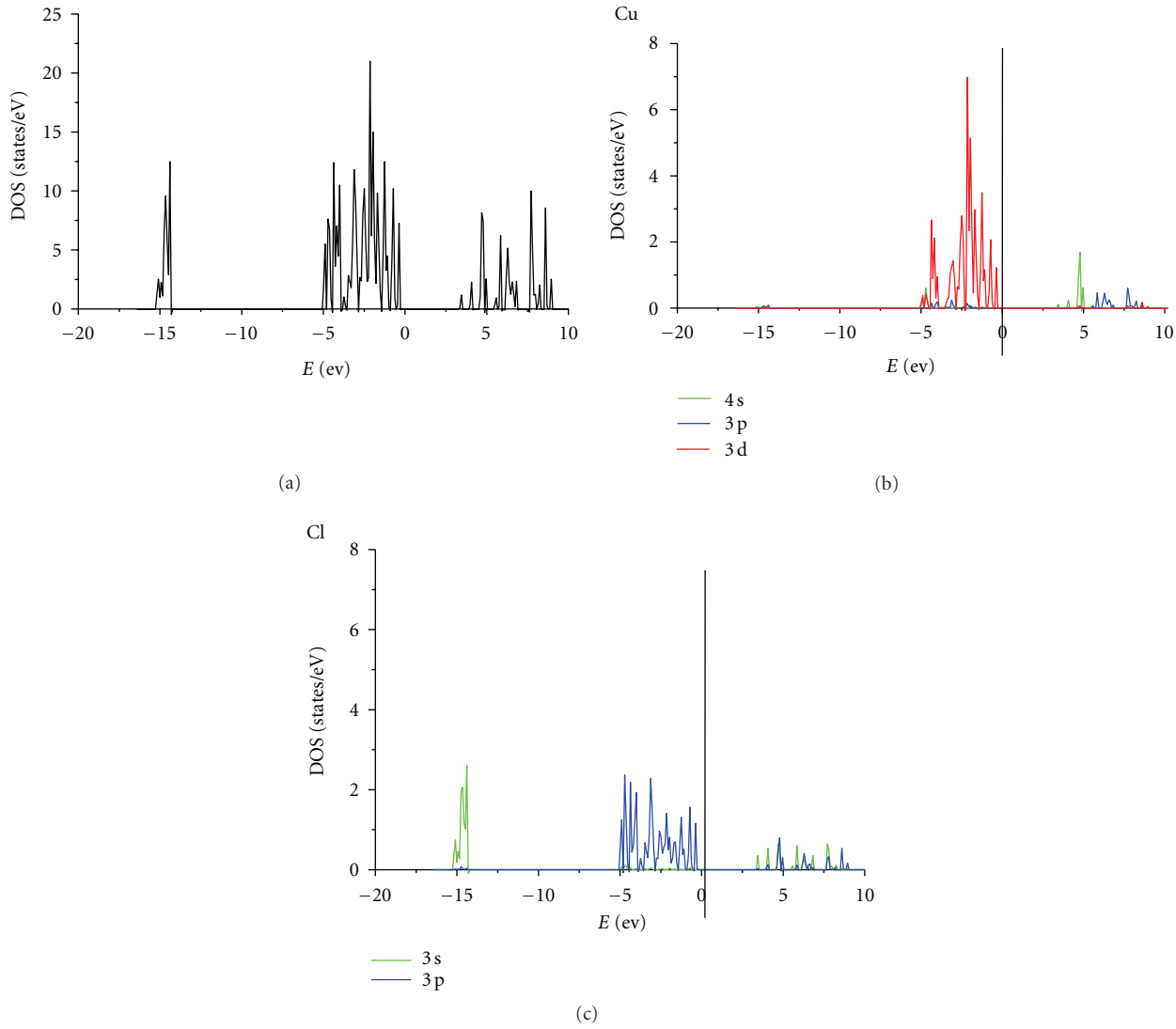

Figure 2: Density of state (DOS) of the bulk of the $CuCl_2$; (a) total DOS, projected DOS (PDOS) of (b) Cu atom and (c) Cl atom.

Test is performed using automatic generation of $(3 \times 3 \times 1)$ and $(5 \times 5 \times 1)$ k-point set of Monkhorst and Pack. For each optimization using these two schemes, the total energy was converged to an accuracy of 1×10^{-3} eV and the forces on each ion to an accuracy of 0.015 eV Å^{-1}. A test using $(5 \times 5 \times 1)$ k-point changed the total energies of the $(3 \times 3 \times 1)$ k-point by a only few meV. All the calculations discussed here are using a $3 \times 3 \times 1$ k-point grid (unless otherwise specified).

Transformation upon building the surface can be viewed in terms of the relaxation, that is, the change in interatomic distances and angle B between optimized bulk unit cell and the extended surface. We found that Cu-Cl distances become longer in the extended surface than the bulk one by only 0.009 Å. While the angle B on the unit cell unit cell varies between 117° in the bulk and 111.3° in the surface (as shown in Figure 3). It is worthwhile also mentioning that optimized surface retains the symmetry exhibited by the unit cell. A noticeable difference in c and a lattice constants could be rationalized based on the shortcoming of standard DFT methods in descrying states relating to long-term weak interactions (Van der Walls type) [33, 34].

The surface has a space group C2/m (as shown in Figure 3) the same as that of the $CuCl_2$ bulk. Unit cells are shifted from each other by 4.06 Å. The super-cell of the surface is illustrated in Figure 4; the top and side views are also shown in Figure 5. All bond lengths and bond angles are illustrated in Table 2 based on Figure 5(b). The distance between each two atomic layer is 3.212 Å. The surface has been optimized also by the $(5 \times 5 \times 5)$ k-point set, and some of the bond lengths and bond angles are illustrated also in Table 2 based on Figure 5(b). As can be noticed from Table 2,

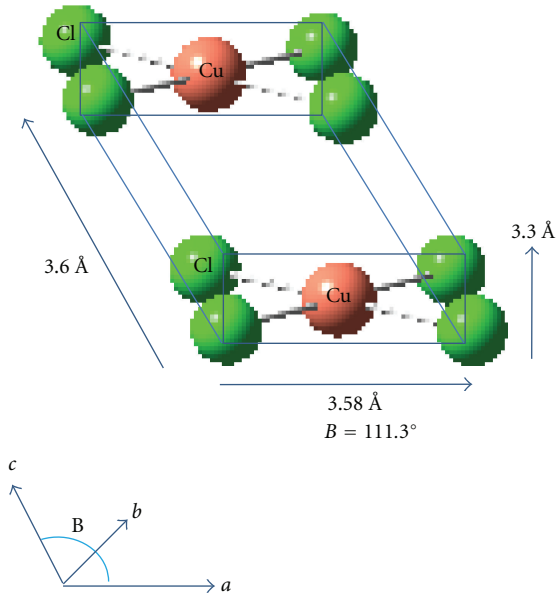

FIGURE 3: the unit-cell of the $CuCl_2(100)$ surface: it is distorted in the (c) direction, which represents the height. In online version, green circles represent Cl atoms, while red circles represent Cu atom.

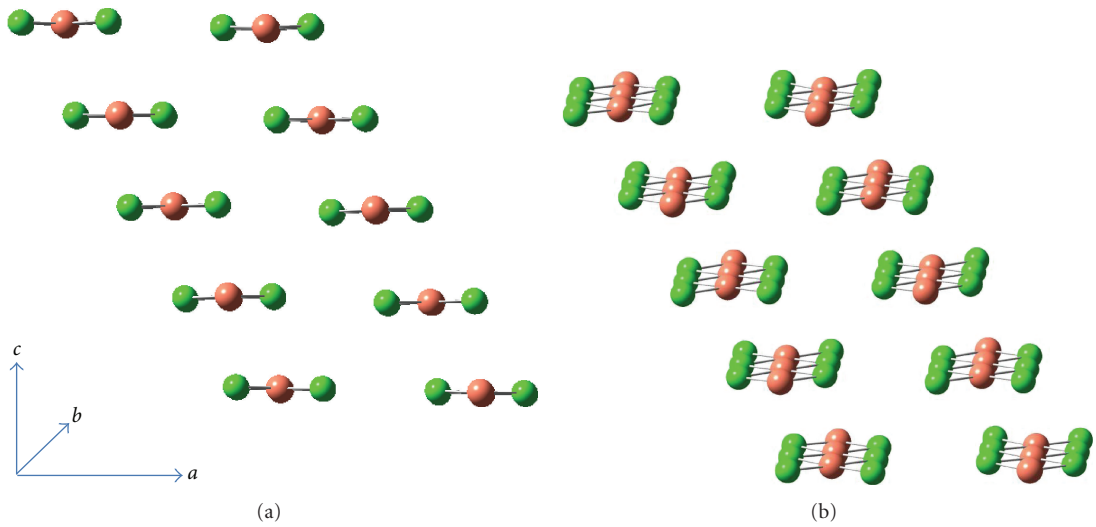

FIGURE 4: (a) Side view of the (2×2) unit-cell of the $CuCl_2(100)$ surface and (b) side view of the (2×2) unit-cell of the $CuCl_2(100)$ surface but the atoms in Figure 4(b) are rotated with small angle to show the atoms in each layer. The (b) direction is perpendicular to both (a) and (c). The unit-cell is distorted in the (c) direction, which represents the height.

some of the bond length shrinks slightly by 0.02 Å while the others stay the same. Also some of the bond angle did not change, while the others changed by only 0.2°. Angle B in the unit cell illustrated in Figure 3 becomes smaller also by 0.8°.

3.3. Electronics Properties. The electronics properties of the $CuCl_2(100)$ surface are investigated by calculating the density of state (DOS) for a slab containing five layers using the automatic generation of $(3 \times 3 \times 1)$ k-point. Figure 6 shows the total DOS and projected DOS of the surface. The investigation of the DOS shows that there are three main regions in the valence band below the Fermi level (0 eV in Figure 6(a)). The first and second regions occupy the regions of (−2 to −6) eV and (−6 to −8) eV. These two regions are manly composed of Cu 3d (Figure 6(b)), with a little contribution of Cl 3p, but the Cu (4s and 3p) and Cl 3s states are minimal (Figures 6(b) and 6(c)).

The last region in the valence band is starting at −17 eV; it is composed of Cl 3s states. The conduction band has

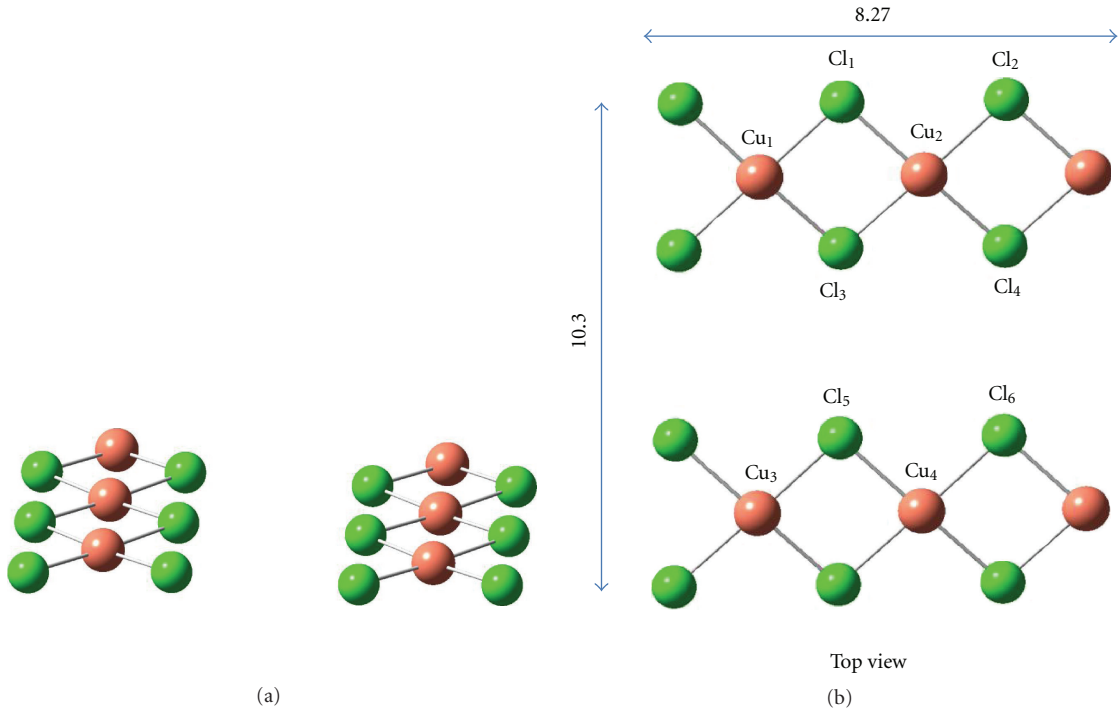

FIGURE 5: (a) Side view and (b) top view of the $CuCl_2(100)$ surface; Figure 5(a) shows part of the surface in Figure 5(b) but rotated to show the structure. Dimensions are in angstrom.

TABLE 2: Calculated structural parameters of the $CuCl_2(100)$ surface using $(3 \times 3 \times 1)$ and $(5 \times 5 \times 1)$ k-point set of Monkhorst and Pack, angle B is the one in the unit cell as in Figure 3.

Bond length (Å)	$(3 \times 3 \times 1)$	$(5 \times 5 \times 5)$	Bond angle (°)	$(3 \times 3 \times 1)$	$(5 \times 5 \times 5)$
Cu_1–Cl_1	2.287	2.275	Cu_1–Cl_1–Cu_2	94	94
Cl_1–Cu_2	2.280	2.273	Cl_1–Cu_2–Cl_2	93.8	94
Cu_1–Cl_3	2.270	2.270	Cl_1–Cu_1–Cl_3	86	86
Cl_3–Cu_2	2.270	2.275	Cu_1–Cl_3–Cu_2	94	94
Cu_1–Cu_3	7.190	7.190	Cl_1–Cu_2–Cl_3	86.2	86
Cl_3–Cl_5	4.090	4.090	B	111.3	110.5
Cu_2–Cu_4	7.190	7.190	—	—	—
Cl_4–Cu_6	4.080	4.080	—	—	—

two distinct regions starting at 1.5 eV with a wide of approximately 2.5 eV for each one. Each of these regions has small peaks at 3.2 eV and 5.2 eV, respectively. The first region is predominantly Cu (4s and 3p) and Cl (3s and 3p), while the second region is predominantly of Cu 4s and the Cl (3s and 3p).

4. Conclusions

The structural, electronic properties of bulk and (100) surface of $CuCl_2$ were investigated by means of periodic quantum chemical calculation based on the first-principle DFT approach. For the bulk, the comparison of optimized structural parameters with experimental and previous DFT study shows that the lattice constants are in a good agreement. The supercell of the $CuCl_2(100)$ surface showed to be axially distorted in the z direction. The interlayer distance, all the bond lengths, and the bond angle are calculated.

Total and projected Density of State (DOS) for the bulk and the extended surface is calculated. For the (100) surface, the valence band is having two regions: the first one composed of Cu (3d) and Cl (3p), while the second region is composed of Cl (3s) states. The surface states above the Fermi level are composed of manly Cu (4s and 3p) and Cl (3s and 3p). An extension to this work is to study the adsorption and dissociation of small molecules such as H_2 and H_2O on this surface.

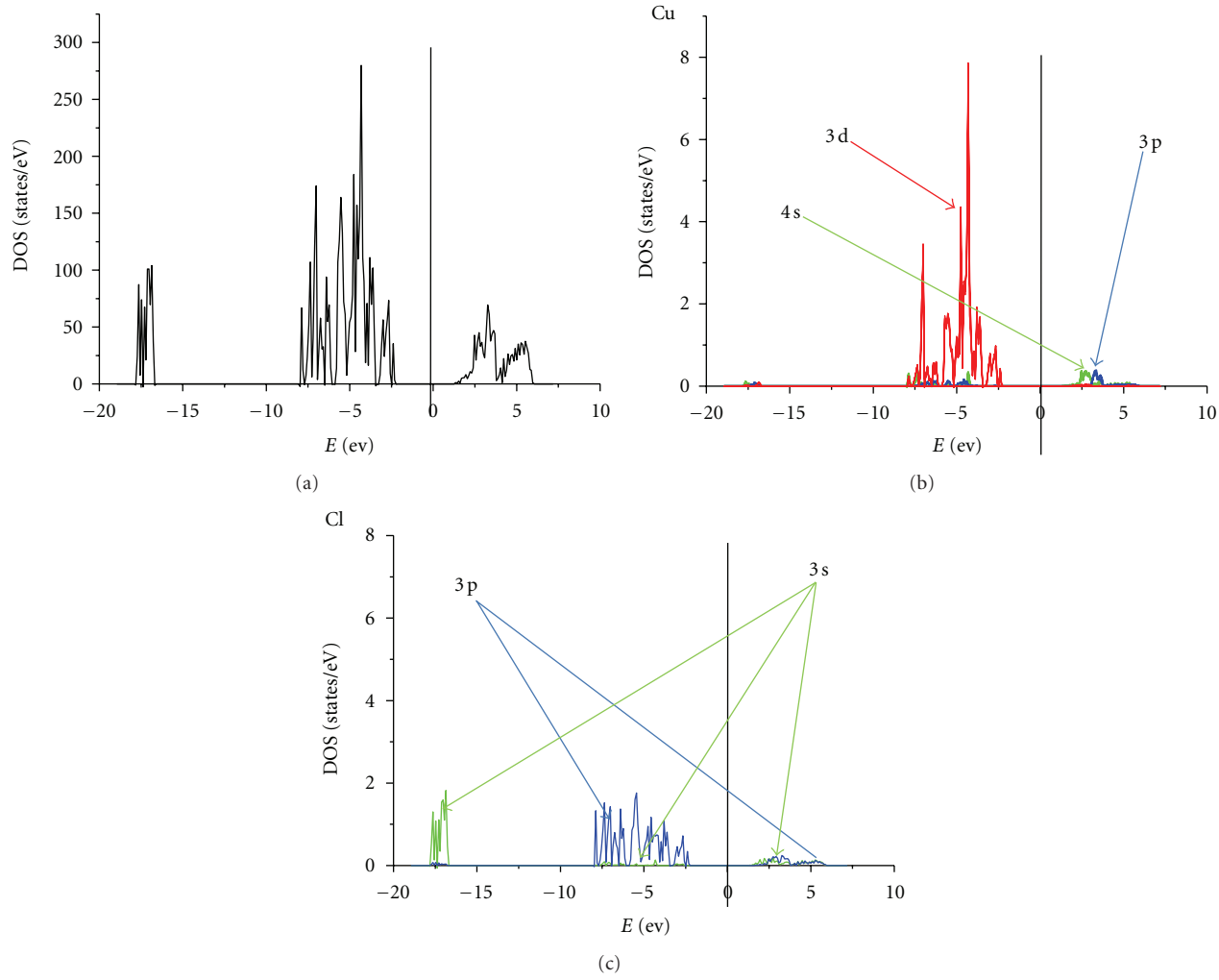

Figure 6: Density of state (DOS) of the $CuCl_2(100)$ surface: (a) total dos, (b) projected DOS (PDOS) of the surface Cu atom, and (c) projected DOS (PDOS) of the surface Cl atom.

References

[1] K. S. Subramanian, "Determination of tin in lead/tin solder leachates from copper piping by graphite platform furnace atomic-absorption spectrometry," *Talanta*, vol. 36, no. 11, pp. 1075–1080, 1989.

[2] V. V. Smirnov and J. P. Roth, "Mechanisms of electron transfer in catalysis by copper zinc superoxide dismutase," *Journal of the American Chemical Society*, vol. 128, no. 51, pp. 16424–16425, 2006.

[3] W. F. Paxton, J. M. Spruell, and J. F. Stoddart, "Heterogeneous catalysis of a copper-coated atomic force microscopy tip for direct-write click chemistry," *Journal of the American Chemical Society*, vol. 131, no. 19, pp. 6692–6694, 2009.

[4] J. Song, T. Zhao, and Y. Du, "Supported copper catalysts for direct vapor-phase oxycarbonylation of methanol," *Chinese Journal of Catalysis*, vol. 27, no. 5, pp. 386–390, 2006.

[5] Y. Cen, X. Li, and H. Liu, "Preparation of copper-based catalysts for methanol synthesis by acid-alkali-based alternate precipitation method," *Chinese Journal of Catalysis*, vol. 27, no. 3, pp. 210–216, 2006.

[6] M. H. Looi, S. T. Lee, and S. B. Abd-Hamid, "Use of citric acid in synthesizing a highly dispersed copper catalyst for selective hydrogenolysis," *Chinese Journal of Catalysis*, vol. 29, no. 6, pp. 566–570, 2008.

[7] M. Altarawneh, B. Z. Dlugogorski, E. M. Kennedy, and J. C. Mackie, "Mechanisms for formation, chlorination, dechlorination and destruction of polychlorinated dibenzo-*p*-dioxins and dibenzofurans (PCDD/Fs)," *Progress in Energy and Combustion Science*, vol. 35, no. 3, pp. 245–274, 2009.

[8] P. J. Goddard and R. M. Lambert, "Adsorption-desorption properties and surface structural chemistry of chlorine on Cu(111) and Ag(111)," *Surface Science*, vol. 67, no. 1, pp. 180–194, 1977.

[9] M. F. Kadodwala, A. A. Davis, G. Scragg et al., "Structural determination of the Cu(111)-(3×3) R30°-Cl/Br surface using the normal incidence X-Ray standing wave method," *Surface Science*, vol. 324, no. 2-3, pp. 122–132, 1995.

[10] M. D. Crapper, C. E. Riley, P. J. J. Sweeney, C. F. McConville, and D. P. Woodruff, "Complete adsorption site information for Cl on Cu(111) using X-ray absorption fine structure and

photoelectron diffraction," *EPL (Europhysics Letters)*, vol. 2, no. 11, p. 857, 1986.

[11] D. P. Woodruff, D. L. Seymour, C. F. McConville et al., "Simple x-ray standing-wave technique and its application to the investigation of the Cu(111) ($\sqrt{3}$ $\sqrt{3}$) R30°-Cl structure," *Physical Review Letters*, vol. 58, no. 14, pp. 1460–1462, 1987.

[12] W. K. Way, A. C. Pike, S. W. Rosencrance, R. M. Braun, and N. Winograd, "Coverage-dependent bond length of chlorine adsorbed on Cu(111)," *Surface and Interface Analysis*, vol. 24, no. 2, pp. 137–141, 1996.

[13] T. Sakurai and T. Hashizume, "FI-STM study of metal surfaces," *Nanotechnology*, vol. 3, no. 3, pp. 126–132, 1992.

[14] D. W. Suggs and A. J. Bard, "Scanning tunneling microscopic study with atomic resolution of the dissolution of Cu(111) in aqueous chloride solutions," *Journal of the American Chemical Society*, vol. 116, no. 23, pp. 10725–10733, 1994.

[15] A. Ignaczak and J. A. Gomes, "Interaction of halide ions with copper: the DFT approach," *Chemical Physics Letters*, vol. 257, no. 5-6, pp. 609–615, 1996.

[16] K. Doll and N. M. Harrison, "Chlorine adsorption on the Cu(111) surface," *Chemical Physics Letters*, vol. 317, no. 3–5, pp. 282–289, 2000.

[17] A. Migani, C. Sousa, and F. Illas, "Chemisorption of atomic chlorine on metal surfaces and the interpretation of the induced work function changes," *Surface Science*, vol. 574, no. 2-3, pp. 297–305, 2005.

[18] A. Migani and F. Illas, "A systematic study of the structure and bonding of halogens on low-index transition metal surfaces," *Journal of Physical Chemistry B*, vol. 110, no. 24, pp. 11894–11906, 2006.

[19] S. Peljhan and A. Kokalj, "Adsorption of Chlorine on Cu(111): A Density Functional Theory Study," *The Journal of Physical Chemistry C*, vol. 113, no. 32, pp. 14363–14376, 2009.

[20] L. B. Bergasova and S. K. Filatov, "The new mineral tolbachite $CuCl_2$," *Doklady Akademii Nauk SSSR*, vol. 270, pp. 415–417, 1983.

[21] B. Gmelin, *Handbuch Der Aanorganischen Chemie*, vol. 211, Chemie GmbH, Weinheim, Germany, 1958.

[22] A. F. Wells, "333. The crystal structure of anhydrous cupric chloride, and the stereochemistry of the cupric atom," *Journal of the Chemical Society*, vol. 1, pp. 1670–1675, 1947.

[23] P. C. Burns and F. C. Hawthrone, "Tolbachite, $CuCl_2$, the first example of Cu^{2+} octahedrally coordinated by Cl^-," *The American Mineralogist*, vol. 78, pp. 187–189, 1993.

[24] G. Kresse and J. Hafner, "Ab initio molecular dynamics for liquid metals," *Physical Review B*, vol. 47, no. 1, pp. 558–561, 1993.

[25] G. Kresse and J. Hafner, "Ab initio molecular-dynamics simulation of the liquid-metal–amorphous-semiconductor transition in germanium," *Physical Review B*, vol. 49, no. 20, pp. 14251–14269, 1994.

[26] G. Kresse and J. Furthmuller, "Efficiency of ab-initio total energy calculations for metals and semiconductors using a plane-wave basis set," *Computational Materials Science*, vol. 6, no. 1, pp. 15–50, 1996.

[27] G. Kresse and J. Furthmuller, "Efficient iterative schemes for ab initio total-energy calculations using a plane-wave basis set," *Physical Review B*, vol. 54, no. 16, pp. 11169–11186, 1996.

[28] J. P. Perdew, J. A. Chevary, S. H. Vosko et al., "Atoms, molecules, solids, and surfaces: applications of the generalized gradient approximation for exchange and correlation," *Physical Review B*, vol. 46, no. 11, pp. 6671–6687, 1992.

[29] P. E. Blöchl, "Projector augmented-wave method," *Physical Review B*, vol. 50, no. 24, pp. 17953–17979, 1994.

[30] H. J. Monkhorst and J. D. Pack, "Special points for Brillouin-zone integrations," *Physical Review B*, vol. 13, no. 12, pp. 5188–5192, 1976.

[31] D. R. Lide, Ed., *CRC Handbook of Chemistry and Physics*, CRC Press, Boca Raton, Fla, USA, 7th edition, 1993.

[32] J. Find, D. Herein, Y. Uchida, and R. Schlögl, "New three-dimensional structural model for the $CuCl_2$ graphite intercalation compound," *Carbon*, vol. 37, no. 9, pp. 1431–1441, 1999.

[33] M. Altarawneh, M. W. Radny, P. V. Smith, J. C. Mackie, E. M. Kennedy, and B. Z. Dlugogorski, "2-Chlorophenol adsorption on Cu(1 0 0): first-principles density functional study," *Surface Science*, vol. 602, no. 8, pp. 1554–1562, 2008.

[34] O. A. Lilienfeld, I. Tavernelli, U. Rothlisberger, and D. Sebastiani, "Optimization of effective atom centered potentials for London dispersion forces in density functional theory," *Physical Review Letters*, vol. 93, no. 15, Article ID 153004, 2004.